HHS Public Access

Acupuncture Activates a Direct Pathway from the Nucleus Tractus Solitarii to the Rostral Ventrolateral Medulla

Zhi-Ling Guo and **Shaista Malik**

Department of Medicine and Susan Samueli Integrative Health Institute, School of Medicine, University of California, Irvine, Irvine, CA 92697, USA

Abstract

Our previous studies have shown that electroacupuncture (EA) at the Jianshi-Neiguan acupoints (P5–6, overlying the median nerve) attenuates sympathoexcitatory responses through its influence on neuronal activity in the rostral ventrolateral medulla (rVLM). The nucleus tractus solitarii (NTS) receives input from somatic nerve stimulation. Connections between the NTS and the rVLM during EA stimulation have not been investigated and thus were the focus of the present study. Seven to ten days after unilateral microinjection of a rhodamine-conjugated microsphere retrograde tracer (100 nl) into the rVLM, rats were subjected to EA or sham-EA without electrical stimulation. EA was performed for 30 min at the P5–6 acupoints bilaterally. Perikarya containing the microsphere tracer were found in the NTS of both groups. Compared to controls (needle placement without electrical stimulation, n=7), c-Fos immunoreactivity and neurons double-labeled with c-Fos, an immediate early gene, and the tracer were significantly increased in the NTS of EA-treated rats (all P<0.05; n=8), particularly, in the medial and lateral subdivisions of NTS at subpostremal and obex levels. These results suggest that EA at the P5–6 acupoints activates NTS neurons. Furthermore, EAactivated NTS neurons directly project to the rVLM and likely influence the rVLM activity.

Keywords

acupuncture; somatic nerve; c-Fos; neural pathways; brain stem

1. Introduction

Stimulating acupoints and underlying neural pathways by acupuncture can be used to deliver targeted therapy for a number of diseases, including hypertension (Longhurst, 2010; Zhao,

Address for correspondence: Zhi-Ling Guo, M.D., Ph.D., Department of Medicine, C240 Medical Science 1, University of California, Irvine, Irvine, California 92697-4075, U.S.A., Tel: 949-824-8161, Fax: 949-824-2200, zguo@uci.edu.

Conflict of Interest
The authors declare no potential conflicts of interest.

2008). Acupuncture application as an integrative medical therapy is accepted increasingly in the Western countries (Longhurst, 2010). However, the neurophysiological mechanisms underlying these therapeutic effects are still largely unknown. The Jianshi-Neiguan acupoints (P5–6), near the wrist of the forearm overlying the median nerve, are used commonly to manage cardiovascular disorders (Longhurst, 2010; Ho et al., 1999). We have shown previously that electroacupuncture (EA) at the P5–6 acupoints reduces sympathoexcitatory responses, in part, through its influence on multiple brain regions, such as the arcuate nucleus in the hypothalamus, ventrolateral periaqueductal gray in the midbrain and raphé nuclei in the brain stem, among others (Li et al., 2006; Tjen-A-Looi et al., 2006; Moazzami et al., 2010; Tjen-A-Looi et al., 2004). Activation of these nuclei during EA ultimately inhibits sympathetic premotor neurons in the rostral ventral lateral medulla (rVLM) and attenuates reflex increases in blood pressure (Li et al., 2009; Tjen-A-Looi et al., 2006; Moazzami et al., 2010), thereby providing an anti-hypertensive response in those with hypertension.

The nucleus tractus solitarii (NTS) is a group of sensory nuclei in the dorsomedial region of the medulla oblongata. The NTS receives and integrates sensory inputs from visceral and somatic nerves and transmits these signals to other regions within the medulla oblongata and other parts of the brain, which subsequently regulate autonomic outflow and a variety of physiological functions including cardiovascular reflex responses (Card, 2011; Anderson, 2011; Tjen-A-Looi et al., 1997; Gao et al., 2011). The activity of cardiovascular-related neurons in the NTS is increased in response to vagal nerve stimulation induced by auricular acupuncture (Gao et al., 2011). However, there is no information available on the mapping of activated neurons in the NTS following application of EA at somatic acupoints like P5–6, which is known to regulate both sympathetic and parasympathetic outflow (Tjen-A-Looi et al., 2006; Moazzami et al., 2010; Tjen-A-Looi et al., 2012b).

Anatomical evidence has shown direct projections from NTS to rVLM (van Bockstaele et al., 1989; Ross et al., 1985; Aicher et al., 1996). In addition, EA at ST-25, an acupoint located 50 mm lateral to the umbilicus on the abdomen in humans, increased c-Fos immunopositive cells in the NTS as well as in the rVLM in the rat, suggesting a potential interaction between these two nuclei during EA stimulation (Iwa et al., 2007). However, it is unknown if NTS neurons activated by EA at the P5–6 acupoints directly synapse with rVLM neurons.

Thus, the present study examined whether EA at the P5–6 acupoints activates NTS neurons by assessing its expression of c-Fos, an immediate early gene, serving as a molecular marker of neuronal activation. The present study also identified pathways between the NTS and the rVLM during application of EA at P5–6. Taken together, we hypothesized that EA at the P5–P6 acupoints activates neurons in the NTS, some of which directly project to the rVLM.

2. Results

2.1. Neurons labeled with retrograde tracer in the NTS

The microinjection site of the retrograde tracer was found inside the rVLM in 15 out of 21 rats. The locations of injected tracer in the medulla closely matched the coordinates of the

rVLM as defined by Paxinos and Watson's atlas for the rat (Paxinos and Watson, 2009). As demonstrated in the Fig.1(Panel A and B1–3), the microinjection sites in the rat were located 12.0 to 12.48 mm caudal to bregma, 2.0–2.6 mm lateral from the midline and 0.2–0.7 mm from ventral surface of the medulla. They were lateral to the paragigantocellularis nucleus, ventral to the Botzinger complex, and medial to the VII cranial nucleus at the high rostral level (Paxinos and Watson, 2009; Li et al., 2009). In these 15 animals subjected to EA or sham-EA, we consistently observed that neurons labeled with the retrograde microsphere tracer were distributed rostrally and caudally throughout the NTS when the tracer was deposited in the rVLM. The labeled neurons were located in the commissural, medial, ventral and lateral subdivisions of NTS, mainly at levels from Bregma –12.6 to –15.0 mm (Paxinos and Watson, 2009). Approximately two-thirds of the neurons labeled with microspheres in the NTS were found to be located ipsilateral to the injection site in the rVLM. Fig. 1 demonstrates low and high power fluorescent images of neurons labeled with the microsphere tracer in the NTS following injection of the retrograde tracer in the ipsilateral rVLM. The distribution of the tracer-labeled neurons in the NTS was similar in EA-treated and control rats (Figs. 1 and 2, and Table 1).

2.2. c-Fos immunoreactivity in the NTS

C-Fos positive cells were found in the NTS of control and EA-treated rats (Fig. 1). Thus, we systemically examined c-Fos immunoreactivity at multiple levels of the NTS rostrocaudally according to Paxinos & Watson's atlas (Paxinos and Watson, 2009). Sections were selected from five different levels of the NTS for further evaluation (Figs. 2 and 3). They represented the rostral, intermediate, subpostrema, obex and caudal levels as shown in Fig. 2, generally matching sections from Bregma –12.6, –13.2, –13.8, –14.4 and –15.0 mm, respectively (Paxinos and Watson, 2009; Lin and Talman, 2002). We observed that Fos-labeled neurons in the NTS of EA-treated rats (n=8) were approximately two to five times greater than controls (n=7), considering the entire rostral-caudal extension of the NTS (Fig. 3 and Table 1). More specifically, Fos-positive neurons were increased significantly in the intermediate, subpostrema, obex and caudal regions of the NTS in the EA group, compared to the sham-EA group (all $P<0.05$; Fig. 3 and Table 1).

To further assess EA-related responses in subdivisions of the NTS throughout its rostrocaudal extension, we divided each level of the NTS into its lateral (including dorsal and ventrolateral), ventral, medial (including dorsomedial and intermediate) and commissural regions (Fig. 2), based on Paxinos & Watson's atlas (Paxinos and Watson, 2009). As demonstrated in Fig. 3, compared to controls, EA-induced significant increases in c-Fos immunoreactivity in the lateral NTS at the subpostrema, obex and caudal levels, ventral NTS at the subpostrema and obex levels, and medial NTS at the rostral, subpostrema, obex and caudal levels (all $P<0.05$). The commissural region of the NTS is located at the subpostrema level and more caudally. There were more cFos positive cells in this part of the NTS at the subpostrema, obex and caudal levels in the EA-treated group, in comparison with the control group (all $P<0.05$; Fig. 3). In particular, EA increased the number of c-Fos positive neurons in all NTS subdivisions at the subpostrema and obex levels.

2.3. NTS neurons co-labeled with retrograde tracer + c-Fos

Neurons double-labeled with c-Fos nuclei and the retrograde tracer were found in the NTS rostral-caudally in both EA-treated and control rats (Figs. 1 and 2). However, as shown in Fig. 3 and Table 1, compared to controls, the double-labeled neurons were significantly increased throughout the NTS in the EA-treated rats (all P<0.05), ranging from intermediate to caudal levels (Bregma −13.2, −13.8, −14.4 and −15.0 mm). Notably, they were observed more frequently in all subdivisions of NTS, including the lateral, ventral and medial portions at these levels in the EA-treated group. Also, more doublelabeled neurons were found in the commissural region of the NTS at the subpostrema, obex and caudal levels in animals treated with EA than that in controls (all P<0.05; see Fig. 3 for details). Moreover, in general, the proportion of the double-labeled neurons to the neurons only labeled with the retrograde tracer in the NTS was 13% in the EAtreated group, significantly greater than that (3%) in the control group (P<0.01; Table 1). This high proportion of the double-labeled cells relative to rVLM projecting neurons was especially noted in the NTS between the intermediate and caudal regions (Table 1). Approximately half (51%) of the c-Fos positive NTS neurons co-localized with the retrograde tracer originated from the rVLM of EA-treated rats, a number significantly higher than that in the controls (about 30%, P<0.01; Table 1)

3. Discussion

We have shown previously that somatic EA at the P5–6 acupoints (overlying the median nerve) lowers elevation in blood pressure through modulation of rVLM activity (Tjen-A-Looi et al., 2006; Moazzami et al., 2010; Li et al., 2009). The NTS is an important brain site that receives sensory inputs from both visceral and somatic nerves (Card, 2011; Anderson, 2011; Tjen-A-Looi et al., 1997; Gao et al., 2011). However, it is unclear if EA at the P5–6 acupoints activates NTS neurons, which then directly influence the rVLM. The present study, for the first time, systemically mapped NTS neurons activated by EA at P5–6 and their direct projections to the rVLM. We found that 30 min of EA at the P5–6 acupoints causes c-Fos expression in the multiple subdivisions of NTS throughout their rostro-caudal extensions. Furthermore, EA-induced c-Fos positive neurons in the NTS co-localized with retrogradely transported microspheres originated from the rVLM. As such, our new findings provide evidence showing that EA at the P5–6 acupoints activates NTS neurons that send projections to the rVLM, suggesting potential mechanisms of EA modulation of sympathetic outflow.

C-Fos, an immediate early gene, is rapidly but transiently expressed following cellular stimulation (<5 h) and serves as a molecular marker to identify neuronal activation (Guo et al., 2004; Guo et al., 2002). Care was taken to minimize the expression of c-Fos in the brain induced by non-specific stimuli, including anesthesia and surgical procedures as we described in the Methods section. In this regard, the survival surgical procedure for microinjection of retrograde tracer was conducted at least seven days prior to EA stimulation. In addition, rats were allowed to stabilize for 4 h after acute minor surgery, before treatment with EA. Most importantly, EA and sham-EA were performed with only one difference between them, i.e., with or without electrical stimulation with acupuncture

needles positioned at the P5–6 acupoints. Thus, compared to controls, the pattern of increased c-Fos in the EA-treated rat was caused exclusively by electrical stimulation of needles placed in the P5–6 acupoints rather than by other non-specific stimuli. Like many other studies using c-Fos immunohistological staining, we previously have demonstrated that EA activates neurons in several medullary nuclei including rVLM, caudal ventrolateral medulla, and raphe nuclei, by evaluating their Fos expression (Guo et al., 2004; Guo et al., 2008).

The NTS serves a number of functions linking sensory inputs from both visceral and somatic nerves as well as vegetative autonomic responses associated with gustatory, respiratory, gastrointestinal, and cardiovascular regulations (Card, 2011; Anderson, 2011; Tjen-A-Looi et al., 1997; Gao et al., 2011). The organization of the NTS is a complex network of excitatory and inhibitory neurons that integrate sensory input, and then transmit the signals to other areas of the brain (Card, 2011; Anderson, 2011; van Bockstaele et al., 1989). Using c-Fos immunoreactive labeling, previous studies have demonstrated activation of NTS in response to facial acupuncture or acupuncture used for managing gastrointestinal disorders, for instance, ST-25 acupoint located lateral to the umbilicus (Liu et al., 2004; Iwa et al., 2007). In the present study, we found an increase in c-Fos expression in the NTS following EA stimulation of the P5–6 acupoints commonly used to treat cardiovascular diseases (Longhurst, 2010), suggesting that the NTS likely is involved in acupuncture-related neural regulation of cardiovascular function. Moreover, these observations are congruent with our recent electrophysiological findings about the participation of NTS neurons in EA-modulated cardiovascular responses in the cat (Tjen-A-Looi et al., 2018). In the physiological experiment, we only examined responses of neurons in a specific portion of the NTS located near the obex following EA at the P5–6 acupoints and their role in modulation of vasodepression and bradycardia (Tjen-A-Looi et al., 2018). In the present study, however, we systemically mapped neurons activated by EA at the P5–6 acupoints in the entire NTS throughout its rostro-caudal extension. In this regard, we identified that EA at P5–6 activates neurons in the lateral, ventral, medial and commissural NTS at multiple levels, including the subpostrema, obex and caudal levels except for the rostral NTS that serves more of a role in mediating gustatory function (Loewy and Spyer, 1990). These new anatomical data further suggest the multiple portions of the NTS may contribute to EA-modulation of cardiovascular responses, which warn further investigations.

A previous study showed that EA at ST-25 activates both the NTS and rVLM (Iwa et al., 2007). Direct pathways from the NTS to the rVLM exist (van Bockstaele et al., 1989; Ross et al., 1985; Aicher et al., 1996). These observations suggest the potential for interaction between the NTS and rVLM during acupuncture (Iwa et al., 2007). The rVLM contains presympathetic neurons that control and maintain cardiovascular function (Kline et al., 2010; Ross et al., 1985). After processing the information, the NTS sends direct projections to a variety of brain regions including the rVLM (Card, 2011; Anderson, 2011). Cells in the NTS that project to the rVLM transmit information related to cardiovascular regulation (Kline et al., 2010; van Bockstaele et al., 1989; Ross et al., 1985). Cells labeled with a retrograde tracer injected into the rVLM are distributed throughout the NTS rostral-caudally (van Bockstaele et al., 1989; Ross et al., 1985; Aicher et al., 1996). To more thoroughly investigate the potential influence of the NTS on the rVLM, the present study evaluated

direct pathways between these two nuclei using a combined c-Fos immunohistochemistry and track tracing approach incorporating retrograde labeling with colored microspheres. We found that cells were labeled with retrograde microspheres in the NTS, following injection into the rVLM, suggesting the possibility of direct projections from the NTS to the rVLM. More interestingly, we observed that more than ten percent of NTS neurons forming connections between the NTS and the rVLM were activated during 30 min of EA at low frequency and low intensity. Furthermore, approximately half of the neurons activated by EA in the NTS were co-labeled with the retrograde tracer from the rVLM. There was no study to determine if direct pathways between the NTS and rVLM were activated by somatic nerve activation, like acupuncture. Thus, our data provide new information on a potentially direct influence of EA-activated NTS neurons on the rVLM through a shortloop pathway in the medulla oblongata.

We also noted that about half of the c-Fos positive neurons activated by EA did not colocalize with the retrograde tracer that was injected into the rVLM. These data suggest that NTS cells activated by somatic input during median nerve stimulation frequently do not project directly to the rVLM. The NTS commonly connects with other brain nuclei, especially caudal ventrolateral medulla (cVLM) that has direct projections to the rVLM (Card, 2011; Anderson, 2011; Dampney, 1994; Kawano and Masuko, 1997). The NTScVLM-rVLM pathway is well-known for an important role in processing cardiovascular baroreflex (Dampney, 1994; Chan and Sawchenko, 1998) Our previous studies have demonstrated that cVLM neurons activated by acupuncture directly project to the rVLM, suggesting a possible involvement of this pathway in EA's action in the regulation of cardiovascular responses (Tjen-A-Looi et al., 2013). Thus, it is possible that EA also modulates cardiovascular responses through direct and/or indirect pathways between NTS and other brain areas, such as cVLM, the arcuate nucleus, ventrolateral periaqueductal gray and raphé nuclei, among others, which have been described in our previous studies (Li et al., 2009; Tjen-A-Looi et al., 2006). These potential neural mechanisms require further study.

In the present study, we observed that low-frequency (2 Hz) and low-intensity (1–4 mA) EA at the P5–6 acupoints did not change basal BP and HR, which were consistent with a number of previous studies in both animal and human subjects (Li et al., 2013; Li et al., 2004; Zhou et al., 2007). However, this type of EA application has been demonstrated to reverse cardiovascular pressor or depressor responses and to maintain BP and HR in normal physiological conditions, suggesting that EA with the parameters used in the present study can effectively affect cardiovascular responses (Li et al., 2013; Li et al., 2004; Zhou et al., 2007; Tjen-A-Looi et al., 2012a). Since EA activates multiple brain nuclei associated with cardiovascular regulation, including rVLM, cVLM, NTS, nucleus ambiguous (NAmb) and raphe nuclei, among others (Li et al., 2013; Tjen-A-Looi et al., 2012a; Moazzami et al., 2010; Longhurst JC., 2012; Tjen-A-Looi et al., 2014), which contribute to either increase or decrease BP and HR (Dampney, 1994), the final integrated outcome of EA in the regulation of BP and HR through modulation of the activity of multiple brain regions is likely maintain BP and HR in the normal physiological conditions, leading to homeostasis of cardiovascular function (Longhurst JC., 2012; Li et al., 2013). It may be an essential reason why EA applied in the normal physiological condition does not cause changes in basal BP and HR. However, this observation does not allow us to exclude any possible contribution of EA-

activated neurons in the cardiovascular-related brain regions to the regulation of cardiovascular function. The results from the present study suggest the effect of EA on the NTS and its relationship to the rVLM. Based on many of our previous studies showing EA's action on cardiovascular responses (Li et al., 2013; Li et al., 2004; Tjen-A-Looi et al., 2012a), the present study implies that NTS-rVLM link is likely involved in EA's regulation of cardiovascular responses. To further confirm our suggestions, more advanced studies will be required. In this regard, for instance, using genetic and virus-tracing approaches, we may examine if basal BP and HR are changed after optogenetically stimulating neurons with c-Fos expression in the NTS or rVLM following acupuncture as well as NTS neurons labeled with retrograde virus originated from the rVLM. The advanced approaches may provide direct evidence showing an important role of a neural circuit from the NTS to the rVLM in EA modulation of cardiovascular function, which may overcome the limitation of the present study.

Besides EA, there are other approaches commonly used to stimulate peripheral nerves in animal and human subjects. They include direct electrical nerve stimulation (DENS) and/or transcutaneous electrical nerve stimulation (TENS). While DENS is performed in the peripheral nerves isolated through surgical procedures using electrodes (Li et al., 1998), TENS is conducted using cutaneous electrode pads without penetration of the skin (Francis and Johnson, 2011). In contrast, EA is accomplished by electrical stimulation of acupuncture needles (without insulation) inserted into acupoint(s). In general, EA is distinguished from other somatosensory autonomic responses by its relative specificity of acupoints like the P5–6 acupoints overlying the median nerve used to treat cardiovascular disorders (Li et al., 2013; Tjen-A-Looi et al., 2004; Longhurst, 2013) There is evidence showing that DENS in the median nerve at or near the P5–6 acupoints generates similar effect like EA (Li et al., 1998; Chao et al., 1999). TENS applied to the skin including P5–6 overlying the median nerve as well as the palm side of the thumb overlying the branch of the median nerve significantly lowered the systolic BP in patients with hypertension (Bang et al., 2018), which is similar to EA's action (Li et al., 2015). These findings suggest that there are similarities between DENS/TENS and EA regarding cardiovascular responses. However, these two types of electric stimulation of peripheral nerves are not precisely equivalent to EA. With this respect, besides different procedures employed for conducting stimulation aforementioned, the current used for EA is higher than for DENS, but much lower than for TENS (Li et al., 1998; Francis and Johnson, 2011; Bang et al., 2018). TENS requires much stronger intensities of stimulation used during EA, as it is not directed at specific locations (acupuncture points) overlying the particular nerve (Francis and Johnson, 2011; Bang et al., 2018). Since TENS has been developed to mimic EA, acupuncture-like TENS is used to indicate this type of stimulation in many other studies (Francis and Johnson, 2011). In the clinic, EA is more practical than DENS that requires invasive procedures and is unwilling for a long-term ambulatory application. As such, we think that a clear indication of DENS, TENS or EA applied for the treatment and study is necessary and appropriate.

In summary, the NTS processes information from multiple sensory afferents. Data from this study provide the first evidence for direct projection of neurons activated by median nerve stimulation at the P5–6 acupoints (c-Fos positive cells) from the NTS to the rVLM, suggesting that a neural pathway from the NTS to the rVLM may be involved in EArelated

regulation of physiological functions including cardiovascular responses. This study advances our understanding of the central neural mechanisms underlying acupuncture's effect on the cardiovascular system.

4. Experimental Procedures

4.1. Microinjection of retrograde tracer into the rVLM

All procedures were carried out in accordance with the Society for Neuroscience and the National Institutes of Health guidelines. The minimum possible number of rats (n=21) was used to obtain reproducible and statistically significant results in this study, as required by the Institutional Animal Care and Use Committee. In addition, every effort was made to minimize discomfort and suffering. Surgical and experimental protocols were approved by the Animal Use and Care Committee at the University of California, Irvine. Adult male Sprague-Dawley rats (350–500 g) were used for microinjection of a retrogradely transported microsphere tracer into the rVLM to evaluate for direct projections from the NTS to the rVLM, as described in detail in our previous studies (Li et al., 2009; Guo and Longhurst, 2010). Briefly, a mixture of ketamine/xylazine (80/12 mg/ml, Sigma) was used to induce (0.3–0.4 ml, i.m) and maintain (0.1–0.2 ml, i.m) anesthesia in the animals. Body temperature was monitored with a rectal probe and was maintained at 37°C. Heart rate and oxygen saturation were monitored using a pulse oximeter (Nonin Medical, Inc. Plymouth, MN USA). Following induction, rats were positioned in a stereotaxic apparatus (David Kopf Instruments). A one inch incision was made to expose the skull. A burr hole (4 mm diameter) was made in the bone so that a glass micropipette could be inserted using the following coordinates: 12.0–12.5 mm caudal from the bregma, 2.0–2.5 mm from the midline, and 8.5 mm deep from the dural surface (Paxinos and Watson, 2009; Li et al., 2009). One hundred nanoliters of a retrogradely transported tracer, rhodamine-labeled fluorescent microspheres in suspension (0.04 μm, Molecular Probes, Eugene, OR), were injected into the rVLM through a glass micropipette. The wound was sutured shut. The microspheres were transported during a 7- to 10-day recovery and maintenance period.

4.2. Terminal experimental procedures

Terminal procedures occurred 7 to 10 days after administration of the retrograde tracer. Rats were re-anesthetized with ketamine/xylazine, as described above. An adequate depth of anesthesia was maintained as judged by the stability of respiration, blood pressure, heart rate and the lack of a withdrawal response to toe pinch. A femoral artery and vein were cannulated for measuring arterial blood pressure (BP, Statham P 23 ID, Oxnard, CA, USA) and administering drugs and fluids, respectively. Heart rate (HR) was derived from the arterial pressure pulse with a biotach (Gould Instrument, Cleveland, OH, USA). The animal was ventilated artificially through a cuffed endotracheal tube after intubation. Arterial blood gases and pH were monitored with a blood gas analyzer (Radiometer, Inc., Model ABL-3, Westlake, OH, USA). They were kept within normal limits (PO_2, 100–150 mm Hg; PCO_2, 28–35 mm Hg; pH, 7.35–7.45) by adjusting the volume and/or the ventilation rate, enriching the inspired O_2 supply and administration of 1 M $NaHCO_3$. Body temperature was maintained at 36–38 °C by a water heating pad and a heat lamp.

After the rats were stabilized for 4 h following surgical preparation, pairs of stainless steel, 38-gauge (0.18 mm × 13 mm) acupuncture needles were inserted bilaterally at the P5–P6 acupoints, overlying the median nerves. The P5–P6 acupoints on both forelimbs of small animals are analogous to those in humans (Hua, 1994). The needles without insulations were connected to a constant current stimulator with a stimulus isolation unit and stimulator (Grass, model S88, W. Warwick, RI, USA). Each set of electrodes was stimulated separately so that current did not flow from one location to the contralateral side. The correct location of acupuncture needles in these acupoints was confirmed by observing moderate, repeated paw flexion to achieve a stimulus intensity that just achieved motor threshold induced by EA using low frequency and current (0.5 ms pulses, 2 Hz, 1–4 mA) in each forelimb (Li et al., 1998; Guo and Longhurst, 2010; Zhou et al., 2005a). Subsequently, gallamine triethiodide (4 mg/kg) was administered intravenously to prevent muscle movement during stimulation of somatic nerves. The previous study showed that EA at P5–6 acupoints generates similar effects on cardiovascular responses like direct stimulation of median nerve at or near these acupoints (Li et al., 1998; Chao et al., 1999).

4.3. Experimental protocols

Rats subjected to microinjection of the retrograde tracer into the rVLM were divided randomly into an EA-treated group and a sham-EA group. As applied in our previous studies (Guo and Longhurst, 2010; Zhou et al., 2005a), low-frequency, low current EA (0.5 ms pulses, 2 Hz, 2–5 V, 1–4 mA) was administered for 30 min in the present investigation. In control animals, acupuncture needles (diameter: 0.16 mm) were inserted into the P5–P6 acupoints for 30 min but were not stimulated electrically following placement. Previous studies have demonstrated that this control does not evoke input to the rVLM or modulate sympathetic reflexes and serves as an adequate control for EA (Zhou et al., 2005b; Tjen-A-Looi et al., 2004; Li et al., 2009). There were no changes in basal BP and HR during EA or sham-EA as we have noted previously (Zhou et al., 2007; Li et al., 2004).

4.4. Immunohistochemical staining

4.4.1. Tissue preparation—As described in our previous studies (Guo and Longhurst, 2010; Li et al., 2009), 90 min after termination of EA or the control, deep anesthesia was induced by another larger dose of the ketamine/xylazine (0.5–0.7 ml, i.m.). Transcardial perfusion was performed using 500 ml of 0.9% saline solution followed by 500 ml of 4% paraformaldehyde in 0.1 M phosphate buffer (pH 7.4). The medulla oblongata was harvested and sliced into coronal sections (30 μm) using a cryostat microtome (Leica CM1850 Heidelberger Strasse, Nussloch, Germany). Brain sections were placed serially in cold cryoprotectant solution and were used for immunohistochemical labeling as described below and for identifying sites of microsphere tracer injection. Animals were included for immunohistochemical staining and data analysis if the site for microinjection was found to be in the rVLM, as indicated by a sample shown in Figure 1. In this study, freefloating sections were used for the labeling.

4.4.2. c-Fos immunohistochemical labeling—After washing for 30 min (10 min × 3 times) in phosphate-buffered saline containing 0.3% Triton X-100 (PBST; pH = 7.4), brain sections were placed for 1 h in 1% normal donkey serum (Jackson Immunoresearch

Laboratories, West Grove, PA). The sections were incubated with a primary polyclonal rabbit anti-Fos antibody (1:2,000 dilution, Oncogene research product, Calbiochem, San Diego, CA, USA) at 4°C for 48 h. The tissues subsequently were rinsed three times (10 min for each rinse) in PBST and incubated with a fluorescein-conjugated donkey anti-rabbit (1:200; Jackson Immunoresearch Laboratories) for 24 h at 4°C. Each section was mounted on a slide and was air dried. The slides were coverslipped using the mounting medium (Vector Laboratories, Burlingame, CA). In immunohistochemical control studies, all c-Fos staining was abolished when 1 ml of the diluted primary antibody was preincubated with 5 μg of the immunizing peptide corresponding to amino acids 4–17 of human c-Fos (SGFNADYEASSSRC, Oncogene Research Produc, Calbiochem, #PP10). In addition, no labeling was detected when the primary or secondary antibody was omitted.

4.4.3.   Data analysis—Brain sections were scanned and examined with a standard fluorescent microscope (Nikon, E400, Melville, NY). Two epifluorescence filters (B-2A or G-2A) equipped in a fluorescent microscope were used to identify single stains appearing as green (fluorescein) or red (rhodamine) in brain sections. Sections containing the NTS were identified according to their best matched standard stereotaxic plane, as shown in Paxinos and Watson's atlas for the rat (Paxinos and Watson, 2009). Two sections were selected for each of five representative planes in all animals (Fig. 2).

After examination with the fluorescent microscope, selected sections were further evaluated with a laser scanning confocal microscope (Zeiss LSM 510, Meta System, Thornwood, NY) to confirm the co-localization of two labels. This apparatus was equipped with Argon and HeNe lasers and allowed operation of multiple channels. Lasers of 488- and 543-nm wavelengths were used to excite fluorescein (green) and rhodamine (red), respectively. Digital fluorescent images were captured and analyzed with software (Zeiss LSM) provided with the confocal microscope. Each confocal section analyzed was limited to 0.5 μm thickness in the Z-plane. Images containing two colors in the same plane were merged to reveal the relationship between two labels (see Fig. 1). Single- and double-labeled neurons were evaluated.

The numbers of single- and double-labeled cells in the same section were counted in each animal. The average number of labeled neurons derived from the five representative levels taken from the rostro-caudal extension of the NTS (Fig. 3 and Table 1) was used to represent the average number of neurons per section for statistical analysis (Guo et al., 2004; Guo et al., 2008; Guo et al., 2002).

4.4.4.   Statistical analysis—Data are expressed as means ± SE. All statistical analyses were conducted with statistical software (SigmaStat, Version 3.0, Jandel Scientific Software, San Rafael, CA, USA). The Kolmogorov–Smirnoff test was used to determine if data were normally distributed. Comparisons between two groups were analyzed with the Student's t-test or Mann–Whitney Rank Sum Test. Values were considered to be significantly different when $P<0.05$.

Author Manuscript

Author Manuscript

Author Manuscript

Author Manuscript

Acknowledgments

Abbreviations

BP	Arterial blood pressure
DENS	Direct electrical nerve stimulation
EA	Electroacupuncture
HR	Heart rate
P5–6	Jianshi-Neiguan acupoints
PBST	Phosphate buffered saline containing Triton X-100
NAmb	Nucleus ambiguous
NTS	Nucleus tractus solitarii
TENS	Transcutaneous electrical nerve stimulation
rVLM	Rostral ventrolateral medulla
cVLM	Caudal ventrolateral medulla

Reference List

Aicher SA, Saravay RH, Cravo S, Jeske I, Morrison SF, Reis DJ, Milner TA, 1996 Monosynaptic projections from the nucleus tractus solitarii to C1 adrenergic neurons in the rostral ventrolateral medulla: comparison with input from the caudal ventrolateral medulla. J. Comp Neurol 373: 62–75. [PubMed: 8876463]

Anderson MCaP JFR, 2011 The nucleus of the solitary tract: processing information from viscerosensory afferents In: Llewellyn-Smith IJ, Verberne AJM (Eds.), Central regulation of autonomic functions. Oxford University Press, New York, pp. 23–46.

Bang SK, Ryu Y, Chang S, Im CK, Bae JH, Gwak YS, Yang CH, Kim HY, 2018 Attenuation of hypertension by C-fiber stimulation of the human median nerve and the concept-based novel device. Sci. Rep 8: 14967. [PubMed: 30297735]

Card JPaS AF, 2011 Central autonomic pathways In: Llewellyn-Smith IJ, Verberne AJM (Eds.), Central regulation of autonomic functions. Oxford University Press, New York, pp. 3–22.

Chan RK, Sawchenko PE, 1998 Organization and transmitter specificity of medullary neurons activated by sustained hypertension: implications for understanding baroreceptor reflex circuitry. J Neurosci 18: 371–387. [PubMed: 9412514]

Chao DM, Shen LL, Tjen-A-Looi SC, Pitsillides KF, Li P, Longhurst JC, 1999 Naloxone reverses inhibitory effect of electroacupuncture on sympathetic cardiovascular reflex responses. Am. J. Physiol 276: H2127–H2134. [PubMed: 10362696]

Dampney RAL, 1994 Functional organization of central pathways regulating the cardiovascular system. Physiol. Rev 74: 323–364. [PubMed: 8171117]

Francis RP, Johnson MI, 2011 The characteristics of acupuncture-like transcutaneous electrical nerve stimulation (acupuncture-like TENS): a literature review. Acupunct. Electrother. Res 36: 231–258. [PubMed: 22443026]

Gao XY, Li YH, Liu K, Rong PJ, Ben H, Li L, Zhu B, Zhang SP, 2011 Acupuncture-like stimulation at auricular point Heart evokes cardiovascular inhibition via activating the cardiac-related neurons in the nucleus tractus solitarius. Brain Res. 1397: 19–27. [PubMed: 21596372]

Guo Z-L, Li P, Longhurst J, 2002 Central pathways in the pons and midbrain involved in cardiac sympathoexcitatory reflexes in cats. Neuroscience 113: 433–444.

Guo Z-L, Longhurst JC, 2010 Activation of reciprocal pathways between arcuate nucleus and ventrolateral periaqueductal gray during electroacupuncture: involvement of VGLUT3. Brain Res 1360: 77–88. [PubMed: 20836994]

Guo Z-L, Moazzami AR, Longhurst JC, 2004 Electroacupuncture induces c-Fos expression in the rostral ventrolateral medulla and periaqueductal gray in cats: relation to opioid containing neurons. Brain Res. 1030: 103–115. [PubMed: 15567342]

Guo Z-L, Moazzami A, Tjen-A-Looi S, Longhurst J, 2008 Responses of opioid and serotonin containing medullary raphe neurons to electroacupuncture. Brain Res 1229: 125–136. [PubMed: 18656464]

Ho F-M, Huang P-J, Lo H-M, Lee F-K, Chern T-H, Chiu T-W, Liau C-S, 1999 Effect of acupuncture at Nei-Kuan on left ventricular function in patients with coronary artery disease. Am. J. Chin. Med 27: 149–156. [PubMed: 10467449]

Hua XB, 1994 Acupuncture manual for small animals Experimental acupuncture. Shanghai Science and Technology Publisher, Shanghai, China, pp. 269–290.

Iwa M, Tateiwa M, Sakita M, Fujimiya M, Takahashi T, 2007 Anatomical evidence of regional specific effects of acupuncture on gastric motor function in rats. Auton. Neurosci 137: 67–76. [PubMed: 17884736]

Kawano H, Masuko S, 1997 Synaptic contacts of substance P-immunoreactive axon terminals in the nucleus tractus solitarius onto neurons projecting to the caudal ventrolateral medulla oblongata in the rat. Brain Res. 754: 315–320. [PubMed: 9134991]

Kline DD, King TL, Austgen JR, Heesch CM, Hasser EM, 2010 Sensory afferent and hypoxia-mediated activation of nucleus tractus solitarius neurons that project to the rostral ventrolateral medulla. Neuroscience 167: 510–527. [PubMed: 20153814]

Li P, Ayannusi O, Reed C, Longhurst JC, 2004 Inhibitory effect of electroacupuncture (EA) on the pressor response induced by exercise stress. Clinical Autonomic Research 14: 182–188. [PubMed: 15241647]

Li P, Pitsillides KF, Rendig SV, Pan H-L, Longhurst JC, 1998 Reversal of reflexinduced myocardial ischemia by median nerve stimulation: a feline model of electroacupuncture. Circulation 97: 1186–1194. [PubMed: 9537345]

Li P, Tjen-A-Looi SC., Longhurst JC, 2013 Acupuncture's role in cardiovascular homeostasis In: Xia Ying, Dong Guanghong, Wu Gen-Cheng (Eds.), Current Research in Acupuncture. Springer Science+Business Media, New York, pp. 457–486.

Li P, Tjen-A-Looi SC, Cheng L, Lui D, Painovich J, Vinjanury S, Longhurst JC, 2015 Long-lasting reduction of blood pressure by electroacupuncture in patients with hypertension: randomized controlled trial. Medical Acupuncture 27: 253–266. [PubMed: 26392838]

Li P, Tjen-A-Looi SC, Guo ZL, Fu L-W, Longhurst JC, 2009 Long-loop pathways in cardiovascular electroacupuncture responses. J. Appl. Physiol 106: 620–630. [PubMed: 19074569]

Li P, Tjen-A-Looi SC, Longhurst JC, 2006 Excitatory projections from arcuate nucleus to ventrolateral periaqueductal gray in electroacupuncture inhibition of cardiovascular reflexes. Am. J. Physiol 209: H2535–H2542.

Lin LH, Talman WT, 2002 Coexistence of NMDA and AMPA receptor subunits with nNOS in the nucleus tractus solitarii of rat. J. Chem. Neuroanat 24: 287–296. [PubMed: 12406503]

Liu JH, Li J, Yan J, Chang XR, Cui RF, He JF, Hu JM, 2004 Expression of c-fos in the nucleus of the solitary tract following electroacupuncture at facial acupoints and gastric distension in rats. Neurosci. Lett 366: 215–219. [PubMed: 15276250]

Loewy AD, Spyer KM, 1990 Central regulation of autonomic functions. Oxford University Press.

Longhurst JC., 2012 Acupuncture Regulation of Cardiovascular Function Primer on the Autonomic Nervous System. Elsevier, New York, pp. 653–657.

Longhurst J, 2013 Acupuncture's Cardiovascular Actions: A Mechanistic Perspective. Med. Acupunct 25: 101–113. [PubMed: 24761168]

Longhurst JC, 2010 Acupuncture in Cardiovascular Medicine. In: O' Hara T (Ed.), Integrative Cardiology. Oxford University Press, pp. 100–116.

Moazzami A, Tjen-A-Looi SC, Guo Z-L, Longhurst JC, 2010 Serotonergic projection from nucleus raphe pallidus to rostral ventrolateral medulla modulates cardiovascular reflex responses during acupuncture. J Appl Physiol 108: 1336–1346. [PubMed: 20133441]

Paxinos G, Watson C, 2009 The rat brain in stereotaxic coordinates. Academic Press.

Ross CA, Ruggiero DA, Reis DJ, 1985 Projections from the nucleus tractus solitarii to the rostral ventrolateral medulla. J. Comp Neurol. 242: 511–534. [PubMed: 2418079]

Tjen-A-Looi SC, Li P, Hsiao A-F, Longhurst JC Central processing by electroacupuncture of cardiovascular reflex vasodepression. FASEB. 2012a Ref Type: Abstract

Tjen-A-Looi SC, Bonham A, Longhurst JC, 1997 Interactions between sympathetic and vagal cardiac afferents in nucleus tractus solitarii. Am. J. Physiol 272: H2843–H2851. [PubMed: 9227564]

Tjen-A-Looi SC, Fu LW, Guo ZL, Longhurst JC, 2018 Modulation of Neurally Mediated Vasodepression and Bradycardia by Electroacupuncture through Opioids in Nucleus Tractus Solitarius. Sci. Rep 8: 1900. [PubMed: 29382866]

Tjen-A-Looi SC, Guo ZL, Li M, Longhurst JC, 2013 Medullary GABAergic mechanisms contribute to electroacupuncture modulation of cardiovascular depressor responses during gastric distention in rats. Am. J. Physiol 304: R321–R332.

Tjen-A-Looi SC, Guo ZL, Longhurst JC, 2014 GABA in Nucleus Tractus Solitarius Participates in Electroacupuncture Modulation of Cardiopulmonary Bradycardia Reflex. Am J Physiol Regul Integr Comp Physiol 307: 1313–1323.

Tjen-A-Looi SC, Li P, Longhurst JC, 2006 Midbrain vlPAG inhibits rVLM cardiovascular sympathoexcitatory responses during acupuncture. Am J Physiol 290: H2543–H2553.

Tjen-A-Looi SC, Li P, Li M, Longhurst JC, 2012b Modulation of cardiopulmonary depressor reflex in nucleus ambiguus by electroacupuncture: Roles of opioids and gamma aminobutyric acid. Am J Physiol 302: R833–R844.

Tjen-A-Looi SC, Li P, Longhurst JC, 2004 Medullary substrate and differential cardiovascular response during stimulation of specific acupoints. Am J Physiol 287: R852–R862.

van Bockstaele EJ, Pieribone VA, ston-Jones G, 1989 Diverse afferents converge on the nucleus paragigantocellularis in the rat ventrolateral medulla: retrograde and anterograde tracing studies. J. Comp Neurol 290: 561–584. [PubMed: 2482306]

Zhao ZQ, 2008 Neural mechanism underlying acupuncture analgesia. Prog. Neurobiol 85: 355–375. [PubMed: 18582529]

Zhou W, Fu L-W, Tjen-A-Looi SC, Li P, Longhurst JC, 2005a Afferent mechanisms underlying stimulation modality-related modulation of acupuncture-related cardiovascular responses. J Appl Physiol 98: 872–880. [PubMed: 15531558]

Zhou W, Tjen-A-Looi S, Longhurst JC, 2005b Brain stem mechanisms underlying acupuncture modality-related modulation of cardiovascular responses in rats. J. Appl. Physiol 99: 851–860. [PubMed: 15817715]

Zhou W, Fu L-W, Guo ZL, Longhurst JC, 2007 Role of glutamate in rostral ventrolateral medulla in acupuncture-related modulation of visceral reflex sympathoexcitation. Am J Physiol 292: H1868–H1875.

Highlights

- Electroacupucture at the P5–6 acupoints induces c-Fos expression in the NTS

- NTS neurons are labeled with microsphere retrograde tracer originated from the rVLM

- The rVLM projecting NTS neurons express c-Fos following electroacupucture at P5–6
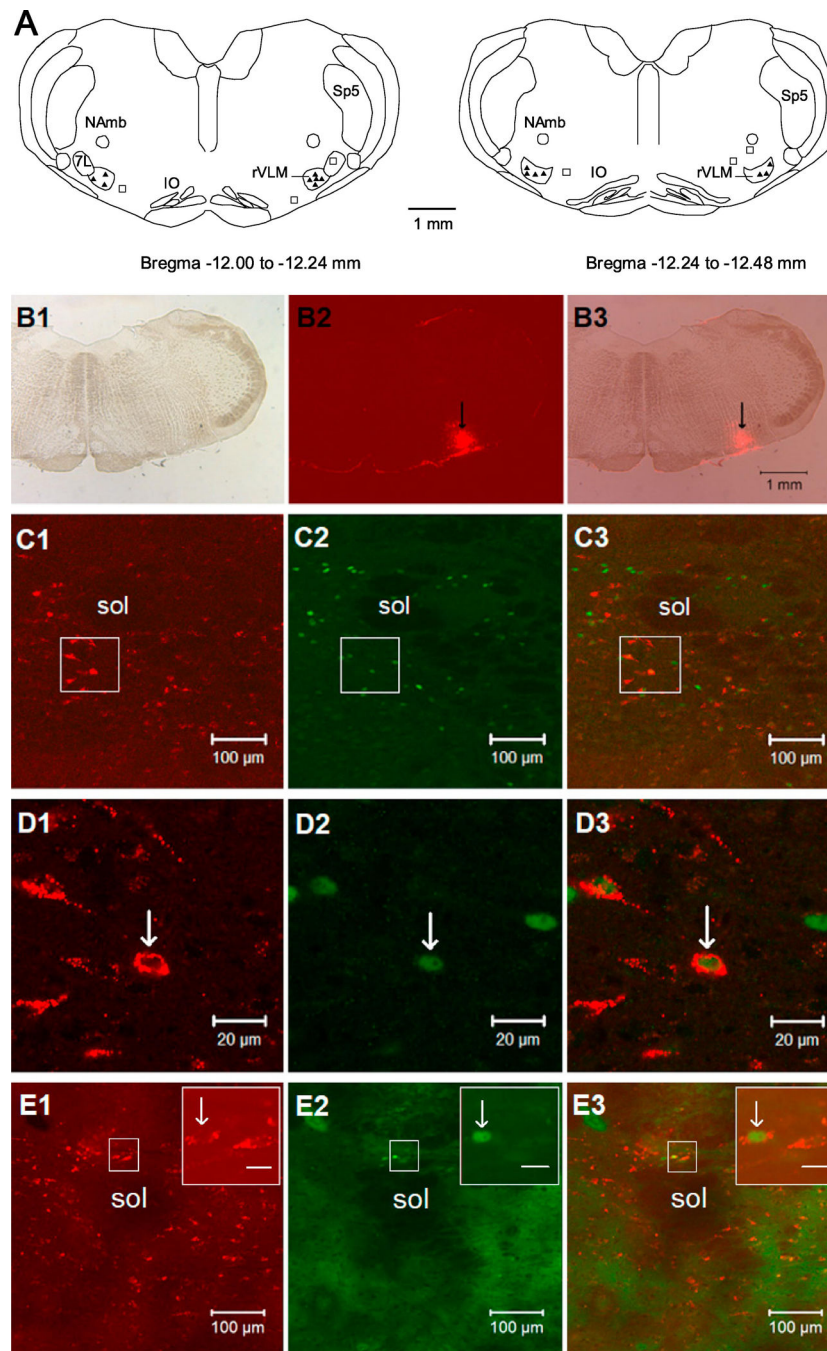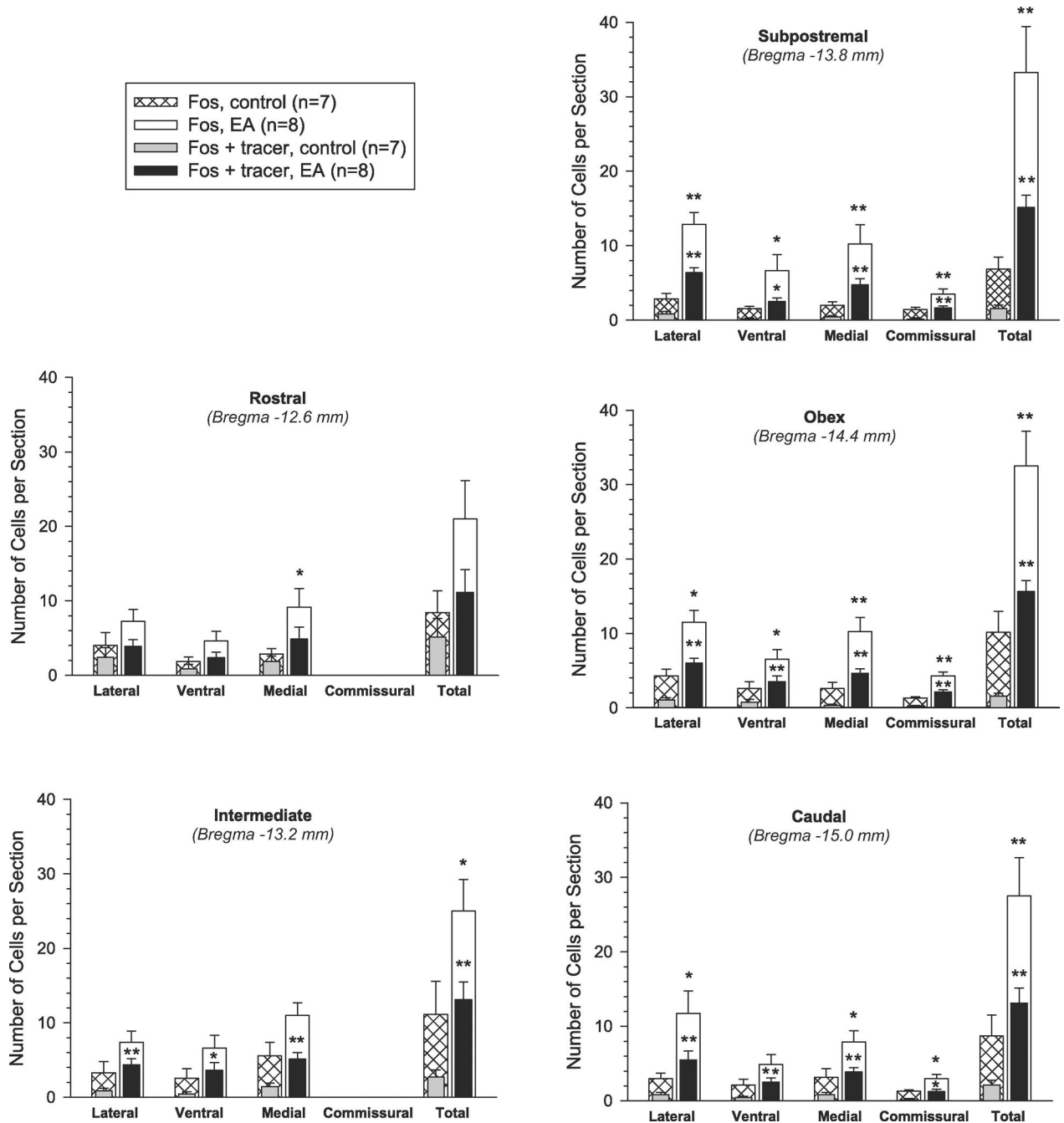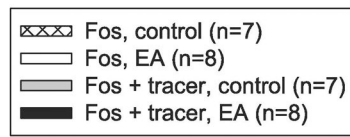
Figure 1.

Microscopic images demonstrating NTS neurons stained with the retrograde microsphere tracer originated from rVLM, c-Fos, and both labels. Panel A: composite maps of rat medulla oblongata displaying histologically verified sites of microinjections of the retrograde microsphere tracer (tracer) into the rVLM of rats. Symbols (▲) and ☐ indicate injection sites inside and outside the rVLM, respectively. All the injections were unilateral (side chosen randomly). Two sections represent levels from Bregma −12.00 to −12.24 mm and −12.24 to −12.48 mm (Paxinos and Watson's rat brain atlas (Paxinos and Watson,

2009)). 7L, facial nucleus; NAmb, nucleus ambiguous; IO, inferior olive; rVLM, rostral ventrolateral medulla; Sp5, spinal trigeminal nucleus. Panels B1–3: microphotographs show an original microinjection site of the tracer in the rVLM (Bregma −12.12 mm). B1: the medulla section under bright field. B2: fluorescent image showing the microinjection site of the tracer in the medulla section. B3: merged image from B1 and B2. Arrows in B2 and B3 indicate the injection site located in the rVLM. Scale bar in B3 represents 1 mm and is applied to B1–3. Panels C1–3: low-power confocal microscopic images show NTS neurons (Bregma −13.80 mm) that are stained with the tracer originated from the rVLM as shown in Panels B1–3, c-Fos, and the tracer + c-Fos in one rat treated with electroacupuncture. C3 is a merged image from C1 and C2. Panels D1–3: magnified regions those are shown within boxes in C1–3 correspondingly. Arrows in D1–3 indicate a neuron labeled with the tracer (red), Fos-positive nucleus (green) and c-Fos + the tracer, respectively. Panels E1–3: low-power confocal microscopic images show NTS neurons (Bregma −13.80 mm) stained with the tracer originated from the rVLM, c-Fos, and the tracer + c-Fos in one rat treated with sham electroacupuncture. E3 is a merged image from E1 and E2. Insets in the upper right corner in E1–3 demonstrate magnified regions those are shown within boxes in E1–3 correspondingly. Arrows in the insets indicate a neuron labeled with the tracer (red), Fos-positive nucleus (green) and c-Fos + the tracer, respectively. Scale bars in C1–3 and E1–3, D1–3, and the insets in E1–3 represent 100, 20, and 10 μm, respectively. Sol, solitary tract; NTS, nucleus tractus solitarii.
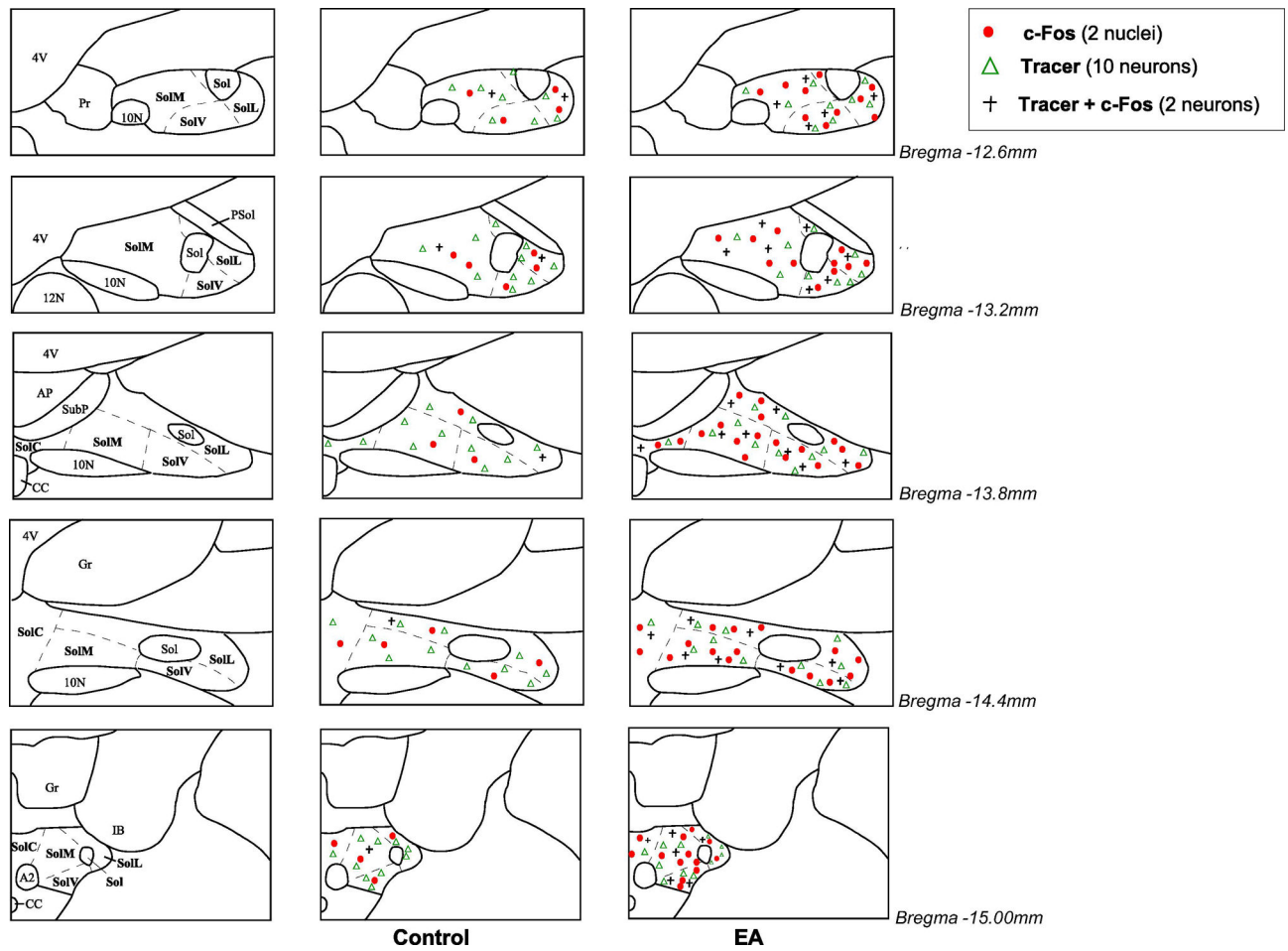
Figure 2.
Distribution of c-Fos immunoreactivity and/or cells labeled with retrograde microsphere tracer (tracer) in the nucleus tractus solitarii (NTS) following electroacupuncture (EA) or sham-EA. Five ipsilateral coronal sections of the NTS following injection of the tracer in the rostral ventrolateral medulla (Paxinos and Watson's atlas (Paxinos and Watson, 2009)) selected from one animal in each experimental group. Each symbol represents labeled cells: , ten cells labeled with the tracer; ●, two c-Fos positive nuclei; +, two neurons co-labeled with c-Fos + tracer.

Figure 3.

Neurons labeled with c-Fos or c-Fos + retrograded microsphere tracer injected into rostral ventrolateral medulla in the lateral, ventral, medial and commissural divisions of nucleus tractus solitarii (NTS) and the entire area of the NTS at multiple rostro-caudal levels. Bars and brackets represent means ± SE. * P<0.05; ** P<0.01, EA (n=8) vs. sham-EA (n=7). EA, electroacupuncture.

Table 1.

C-Fos immunoreactivity and co-location with retrograde tracer in the NTS following electroacupuncture

Level of NTS	Fos cells (#)	Tracer cells (#)	Tracer+Fos cells (#)	Tracer +Fos cells Tracer cells (%)	Tracer +Fos cells Fos cells (%)
Rostral					
(Bregma −12.6 mm)					
Control (n=7)	9 ± 3	96 ± 10	5 ± 3	6 ± 3	49 ± 8
EA-treated (n=8)	21 ± 5	91 ± 8	11 ± 3	11 ± 2	48 ± 7
Intermediate					
(Bregma-13.2 mm)					
Control (n=7)	11 ± 4	111 ± 13	3 ± 1	3 ± 1	27 ± 7
EA-treated (n=8)	25 ± 4 [*]	93 ± 5	13 ± 2 [**]	14 ± 3 [**]	51 ± 5 [**]
Subpostremal					
(Bregma −13.8 mm)					
Control (n=7)	7 ± 2	133 ± 13	2 ± 1	1 ± 1	26 ± 8
EA-treated (n=8)	33 ± 6 [**]	117 ± 9	15 ± 2 [**]	13 ± 1 [**]	49 ± 5 [*]
Obex					
(Bregma −14.4 mm)					
Control (n=7)	10 ± 3	124 ± 15	2 ± 1	1 ± 1	23 ± 8
EA-treated (n=8)	33 ± 5 [**]	114 ± 10	16 ± 2 [**]	14 ± 2 [**]	52 ± 5 [*]
Caudal					
(Bregma −15.0 mm)					
Control (n=7)	9 ± 3	115 ± 10	2 + 1	2 ± 1	24 + 5
EA-treated (n=8)	28 ± 5 [**]	103 ± 9	13 ± 2 [**]	13 ± 2 [**]	50 ± 3 [**]
Average					
Control (n=7)	10 ± 3	116 ± 11	3 ± 1	3 ± 1	30 ± 3
EA-treated (n=8)	28 ± 4 [*]	104 ± 7	14 ± 2 [**]	13 ± 1 [**]	51 ± 4 [**]

Means ± SE. Average number (#) of c-Fos positive cells per section, neurons labeled with retrograde microsphere tracer (tracer) that was injected into rostral ventrolateral medulla and cells co-localized with both stains in the nucleus tractus solitarii (NTS) per section. Also shown are percentages (%) of double-labeled neurons to number of tracer-labeled neurons or Fos positive cells. EA, electroacupuncture stimulation.

[*] P<0.05,

[**] P<0.01; EA-treated group vs. control group.

EA-treated group vs. control group.